

# Determination of topological charges of polychromatic optical vortices

Vladimir Denisenko<sup>1,2</sup>, Vladlen Shvedov<sup>1,3</sup>, Anton S. Desyatnikov<sup>1</sup>,  
Dragomir N. Neshev<sup>1</sup>, Wieslaw Krolikowski<sup>4</sup>, Alexander Volyar<sup>3</sup>,  
Marat Soskin<sup>2</sup>, and Yuri S. Kivshar<sup>1</sup>

<sup>1</sup>*Nonlinear Physics Centre, Research School of Physics and Engineering,  
The Australian National University, Canberra ACT 0200, Australia*

<sup>2</sup>*Institute of Physics, National Academy of Sciences of Ukraine, Kiev, Ukraine*

<sup>3</sup>*Department of Physics, Taurida National University, Simferopol 95007 Crimea, Ukraine*

<sup>4</sup>*Laser Physics Centre, Research School of Physics and Engineering,  
The Australian National University, Canberra ACT 0200, Australia*

**Abstract:** We introduce a simple, single beam method for determination of the topological charge of polychromatic optical vortices. It is based on astigmatic transformation of singular optical beams, where the intensity pattern of a vortex beam acquires a form of dark stripes in the focal plane of a cylindrical lens. The number of the dark stripes is equal to the modulus of the vortex topological charge, while the stripe tilt indicates the charge sign. We demonstrate experimentally the effectiveness of this technique by revealing complex topological structure of polychromatic singular beams.

© 2009 Optical Society of America

**OCIS codes:** (260.1180) Crystal optics, (260.6042) Singular optics

---

## References and links

1. J. F. Nye and M. V. Berry, "Dislocations in wave trains," *Proc. R. Soc. London A* **336**, 165-190 (1974).
2. M. S. Soskin and M. V. Vasnetsov, "Singular optics," *Prog. Opt.* **42**, 219 (Ed. E. Wolf, Elsevier, 2001).
3. M. R. Dennis, K. O'Holleran, and M. J. Padgett, "Singular Optics: Optical Vortices and Polarization Singularities," *Prog. Opt.* **52**, 293 (Ed. E. Wolf, Elsevier, 2009).
4. N. B. Baranova, B. Ya. Zel'dovich, A. V. Mamaev, N. F. Pilipetskii, and V. V. Shkukov, "Dislocations of the wavefront of a speckle-inhomogeneous field (theory and experiment)," *JETP Lett.* **33**, 195-199 (1981).
5. N. R. Heckenberg, R. McDuff, C. P. Smith, and A. G. White, "Generation of optical phase singularities by computer-generated holograms," *Opt. Lett.* **17**, 221-223 (1992).
6. H. I. Sztul and R. R. Alfano, "Double-slit interference with Laguerre-Gaussian Beams," *Opt. Lett.* **31**, 999 (2006).
7. G. Gbur and T. D. Visser, "Coherence vortices in partially coherent beams," *Opt. Commun.* **222**, 117-125 (2003).
8. D. M. Palacios, I. D. Maleev, A. S. Marathay, and G. A. Swartzlander, Jr., "Spatial correlation singularity of a vortex field," *Phys. Rev. Lett.* **92**, 143905 (2004).
9. J. Leach and M. J. Padgett, "Observation of chromatic effects near a white-light vortex," *New J. Phys.* **5**, 154.1-154.7 (2003).
10. O. V. Angelsky, S. G. Hanson, A. P. Maksimyak, and P. P. Maksimyak, "On the feasibility for determining the amplitude zeroes in polychromatic fields," *Opt. Express* **13**, 4396-4405 (2005), <http://www.opticsexpress.org/abstract.cfm?URI=OPEX-13-12-4396>.
11. A. V. Volyar, Yu. A. Egorov, A. F. Rubass, and T. A. Fadeeva, "Fine structure of white optical vortices in crystals," *Tech. Phys. Lett.* **30**, 701-704 (2004).
12. M. S. Soskin, P. V. Polyanskii, and O. O. Arkhelyuk, "Computer-synthesized hologram-based rainbow optical vortices," *New J. Phys.* **6**, 196 (2004).
13. I. Freund, "Poincaré vortices," *Opt. Lett.* **26**, 1996 (2001).
14. V. G. Denisenko, A. Minovich, A. S. Desyatnikov, W. Krolikowski, M. S. Soskin, and Yu. S. Kivshar, "Mapping phases of singular scalar light fields," *Opt. Lett.* **33**, 89-91 (2008).
15. V. Shvedov, W. Krolikowski, A. Volyar, D. N. Neshev, A. S. Desyatnikov and Yu. S. Kivshar, "Focusing and correlation properties of white-light optical vortices," *Opt. Express* **13**, 7393-7398 (2005), <http://www.opticsinfobase.org/abstract.cfm?URI=oe-13-19-7393>.

16. L. Allen, M. W. Beijersbergen, R. J. C. Spreeuw, and J. P. Woerdman, "Orbital angular-momentum of light and the transformation of Laguerre-Gaussian laser modes," *Phys. Rev. A* **45**, 8185-8189 (1992).
17. G. Molina-Terriza, J. Recolons, J. P. Torres, and L. Torner, "Observation of the Dynamical Inversion of the Topological Charge of an Optical Vortex," *Phys. Rev. Lett.* **87**, 023902 (2001).
18. J. Serna, F. Encinas-Sanz, and G. Nemeş, "Complete spatial characterization of a pulsed doughnut-type beam by use of spherical optics and a cylindrical lens," *J. Opt. Soc. Am. A* **18**, 1726-1733 (2001).
19. V. H. Denisenko, M. S. Soskin, and M. V. Vasnetsov, "Transformations of Laguerre-Gaussian modes carrying optical vortex and their orbital angular momentum by cylindrical lens," *Proc. SPIE* **4607**, 54-58 (2002).
20. A. Ya. Bekshaev, M. S. Soskin, and M. V. Vasnetsov, "Transformation of higher-order optical vortices upon focusing by an astigmatic lens," *Opt. Commun.* **241**, 237-247 (2004).
21. R. K. Singh, P. Senthikumar, and K. Singh, "Influence of astigmatism and defocusing on the focusing of a singular beam," *Opt. Commun.* **270**, 128-138 (2006).
22. A. Volyar, V. Shvedov, T. Fadeyeva, A. S. Desyatnikov, D. N. Neshev, W. Krolikowski, and Yu. S. Kivshar, "Generation of single-charge optical vortices with an uniaxial crystal," *Opt. Express* **14**, 3724-3729 (2006), <http://www.opticsinfobase.org/abstract.cfm?URI=oe-14-9-3724>.
23. A. V. Volyar and T. A. Fadeeva, "Generation of singular beams in uniaxial crystals," *Opt. Spectrosc.* **94**, 235-244 (2003).
24. D. N. Neshev, A. Dreischuh, V. Shvedov, A. S. Desyatnikov, W. Krolikowski, and Yu. S. Kivshar, "Observation of polychromatic vortex solitons," *Opt. Lett.* **33**, 1851-1853 (2008).

The study of phase dislocations and vortices attracts growing attention because vortices possess unique features common in any field of wave physics. In particular, an optical vortex has transverse power flow circulating around a dark core with vanishing amplitude [1–3]. In paraxial laser beams, the isolated zeros of the electromagnetic field are associated with phase singularities and they are characterized by an integer index, called topological charge  $l$ , indicating the multiplicity of the  $2\pi l$  azimuthal phase ramp [1]. Typical methods to reveal a topological structure of singular beams are based on their interference with a reference beam [4–6]. The resulting interference fringes exhibit a spiral, in the case of a spherical reference wave or a fork, for a plane reference wave. The form of this interference pattern uniquely determines the sign and magnitude of the topological charge. However, the interference methods are difficult to apply in the study of composite beams, such as partially coherent [7,8] and/or polychromatic beams [9–12], because of a diminished resolution of the interference fringes, caused by low coherence and spatial overlap of various spectral components. The same limitation applies when the reference and singular waves are orthogonally polarized [13, 14].

In this work we explore a different method to determine the topological charge of polychromatic spatially coherent vortex beams. This method is somewhat similar to the visualization of a vortex core by focusing for the spatially partially coherent beams [15]. It is based on the *astigmatic transformation* of the beam by a lens converter [16, 17], which transforms an axially symmetric optical vortex beam into an astigmatic beam with strongly deformed vortex core near the focal plane [18, 19]. The method relies on the fact that a monochromatic higher-order optical vortex splits into constituent elementary (charge one) vortices [20, 21] and their number equals to the total topological charge of the original singular beam. At the same time, the core of each elementary vortex is strongly deformed similar to an edge dislocation [17] near the focus of a cylindrical lens. The deformed vortices form extended pattern of tilted dark stripes whose orientation depends on whether the charge of the vortex is positive or negative. By applying the same procedure to each spectral component of a polychromatic beam we can characterize unambiguously its topological structure.

Theoretically, the field focused by a cylindrical lens with focal length  $f$  can be calculated by solving the paraxial wave equation for the collimated input beam on the lens at  $z = 0$ ,  $E = (x/w + isy/w)^{|l|} \exp(-x^2/w^2 - y^2/w^2)$ , multiplied by the lens transmission function,  $t = \exp(-ik_0 y^2/2f)$ . Here  $w$  is the waist of the Laguerre-Gaussian beam,  $l$  is its topological charge,  $s = \text{sign}(l)$ , and  $k_0 = 2\pi/\lambda$  is the free-space wavenumber. In the focal plane  $z = f$  the result can be expressed in terms of a single dimensionless parameter  $p = k_0 w^2/2f$ . For example, the

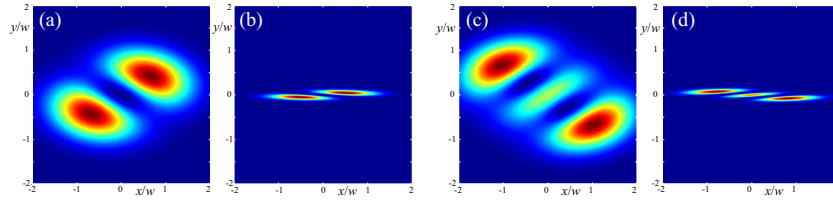


Fig. 1. Intensity patterns in the focal plane of a cylindrical lens calculated for vortex beams with topological charges (a, b)  $l = +1$  and (c, d)  $l = -2$ ; parameter  $p = 1.2$  in (a, c) and  $p = 10.6$  in (b, d).

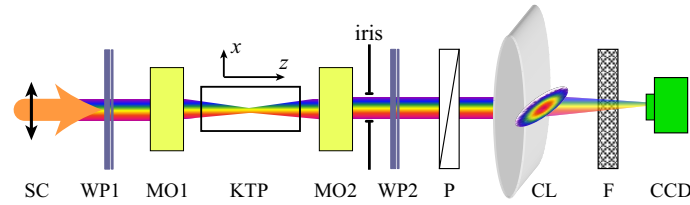


Fig. 2. Experimental setup: SC – supercontinuum beam, WP1 and WP2 – quarter-wave plates; MO1 and MO2 – 3 $\times$  and 5 $\times$  achromatic microscope objectives, respectively; KTP – sample of uniaxial crystal; P – polarizer; F – variable spectral filter (300 – 750 nm); CL – cylindrical lens. The coloring of the beam indicates its polychromatic content.

intensity for single-charge vortex beam, expressed in dimensionless coordinates  $\xi = x/w$  and  $\eta = y/w$ , is given by

$$|E(x, y, z = f)|^2 = p^4 \frac{\xi^2 + 2sp\xi\eta + \eta^2(1 + p^2)}{(1 + p^2)^{3/2}} \exp\left(-\frac{2p^2\xi^2}{1 + p^2} - 2p^2\eta^2\right). \quad (1)$$

We show in Fig. 1 corresponding images for  $l = +1$  (a, b) and  $l = -2$  (c, d), and two values of parameter  $p$ . Note that for large  $p \gg 1$  (as in our experiments below), the intensity distribution is strongly squeezed in  $y$ -direction,  $|E(x, y, z = f)|^2 \simeq p(\xi + sp\eta)^2 \exp(-2\xi^2 - 2p^2\eta^2)$ .

In the experiments, we generate a wide-band supercontinuum beam from a femtosecond laser source and a highly nonlinear photonic crystal fibre. From this continuum, we select a polychromatic beam spanning the spectral range of 450-700 nm. We then generate single [22] and double [11, 23] charge polychromatic vortex beams by using uniaxial crystal in a way similar to that employed in the studies of polychromatic vortex solitons [24] (see Fig. 2). The linearly polarized and highly spatially coherent polychromatic Gaussian beam passes through a quarter-wave plate and is focused by a microscope objective (MO1) into 7 mm long uniaxial  $\text{KTiOPO}_4$  (KTP) crystal. The key element that allows us to switch between single and double charge vortices is the use of polarization transformation in the crystal controlled with the quarter-wave plates WP1, WP2 and the iris diaphragm. After passing through the crystal the beam is re-collimated by a second objective (MO2) and focused by a cylindrical lens (CL) with a focal distance  $l = 50$  mm. The image of the focal caustic of the lens is recorded by a color CCD camera. Due to the very narrow beam size in the focal plane, the observations are made at a short distance after the focal plane to allow the beam expansion due to diffraction. The use of a variable spectral filter (spectral range 300 – 750 nm and bandwidth of 5 nm) before the CCD camera, also enables independent observation of each spectral component of the beam.

We begin with the analysis of single-charge vortices and present our results in Figs. 3(a-f). With the quarter-wave plates WP1, WP2 absent and with the polarizer P set parallel to the linear polarization of the input beam, we generate topological quadrupole of optical vortices at the output of the KTP crystal. As described in Ref. [15], by tilting the optical axis of the

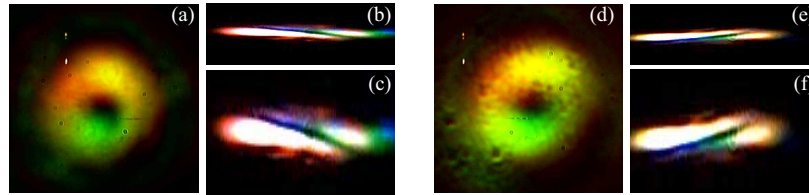


Fig. 3. Vortex beam with topological charge (a-c)  $l = +1$  and (d-f)  $l = -1$ . The original intensity distributions in (a) and (d) to compare with the focal pattern of the cylindrical lens in (b) and (e). The frames (c) and (f) are the images in (b) and (e), respectively, but stretched in vertical direction by a factor of 3.5. The spatial scale is defined by the 5.25 mm size of frames (a) and (d).

KTP crystal ( $\sim 5^\circ$  with respect to the propagation direction) and using the iris diaphragm, we can isolate the single vortex beam of charge  $l = +1$  or  $l = -1$ . These beams are depicted in Fig. 3(a) and 3(d). The white color of intensity profile is achieved by saturation of the camera to visualize the coloring of the tails due to the slight angular dispersion introduced with the tilting of the KTP crystal [24]. Focusing by cylindrical lens results in the patterns shown in Figs. 3(b) and 3(e). They feature one dark stripe across the focal white-light image. The stripes are tilted in the opposite directions for vortices with opposite charges. We note that, in Eq. (1), the dispersion of the field profile is determined by the value of the  $p$  parameter for the different spectral components. For our choice of the spectral range, it varies from  $p = 560$  at  $\lambda = 450$  nm to  $p = 360$  at  $\lambda = 700$  nm. Consequently, the angle of rotation of the dark stripes does not change significantly with the wavelength and the topological structure can be easily determined. Thus for a single-charge vortex beam the results are similar to the case of monochromatic waves [17, 19]. Therefore, in order to determine the topological structure of a single charge polychromatic vortex, we do not need to monitor the individual spectral components of the beam. For better visibility we also show in (c) and (f) the patterns from (b) and (e), respectively, but stretched by 3.5 times in the vertical direction.

Next we generate a double-charge polychromatic vortex beam [11, 23, 24] with the optical axis of the uniaxial KTP crystal oriented parallel to the beam propagation in the setup shown in Fig. 2. In this scheme WP1, WP2 are achromatic (450 – 800 nm) quarter-wave plates that are set to convert the linear polarisation to circular and vice versa. In this way, all spectral components carry the same topological charge  $l = -2$ . The results of our experiments showing the true color profiles of the polychromatic beam and individual spectral components are presented in Fig. 4. Already in the total intensity in (a) the double charge is revealed by the two tilted stripes across the cylindrical focal pattern (bottom). In contrast to the single charge polychromatic vortex, instead of dark stripes, we observe characteristic “rainbow” coloring of the focal pattern. This is due to the fact that the different spectral components are spatially shifted with respect to each other. However, as expected for monochromatic light [20, 21], each of these components undergoes the same polarization conversion in the uniaxial crystal and, as seen in the images (b-h), they carry the same double-stripe patterns.

To demonstrate the simplicity of our method for characterization of polychromatic beams with a complex topological structures, we perform another experiment where we replace (in the arrangement of generation of double-charge polychromatic vortices) the achromatic wave plates with a zero-order monochromatic ones ( $\lambda = 532$  nm). Focusing the output beam by a cylindrical lens results in the transverse intensity distribution shown in Fig. 5(a). Instead of the characteristic two dark stripes expected for a monochromatic beam, we observe no stripes at all (the horizontal stripes in (a) are a residue of the oscillating tails of the beam and white color is due to camera saturation). Such intensity distribution indicates the absence of optical vortices

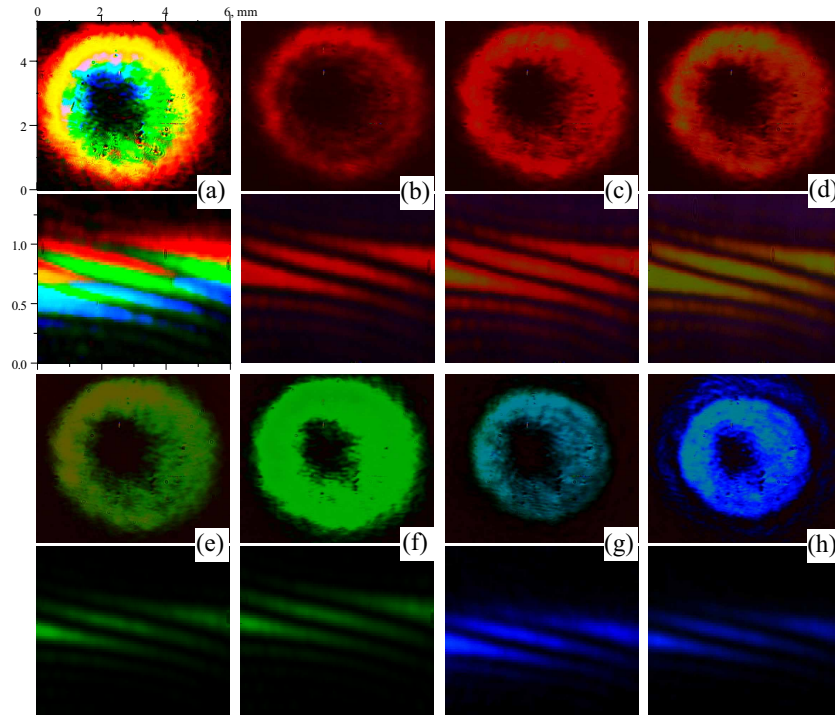


Fig. 4. True colour images of (a) double-charge polychromatic vortex beam and (b-h) its spectral components. After focusing by a cylindrical lens all components form a similar spatial pattern (bottom frames), featuring two distinct dark stripes. The slight colouring in (d,e) is due to the weak peak of transmission of the variable filter at longer wavelengths.

even though there is a clearly pronounced dark spot in the center of the beam. To resolve this apparent contradiction we show in Figs. 5(b-j) the spectrally resolved images of the intensity distribution from Fig. 5(a). These images clearly indicate the topological charge  $l = +2$  in red (b), green (f), and blue (j) components, as seen in the bottom (vertically stretched) images of the cylindrical focal plane. Opposite tilt of the dark stripes, and thus opposite charge  $l = -2$ , is revealed for the spectral components shown in Figs. 5(d, h). In contrast, the components displayed in Figs. 5(c, e, g, i) do not exhibit tilted stripe structure and hence carry zero charge  $l = 0$ . The later conclusion is further supported by the observation of typical “dark cross” pattern in the intensity distribution obtained without the cylindrical lens (top frames).

The explanation of the observed results is the following. Using a monochromatic wave plates with the polychromatic beam results in accumulation of an additional phase by each spectral component. This phase change is proportional to the spectral shift from  $\lambda = 532$  nm and is equivalent to rotation of the polarization of the input and output beams. Therefore, it results in different polarization conversion in the KTP crystal exhibited by the different spectral components. Consequently, some of these components experience transformation to double-charge vortices, while other – to dark cross structures. Because the difference is a continuous function of the wavelength, the transformation from structure (b) to (j) in Fig. 5 is analogous to that experienced by a monochromatic beam with its input polarization being gradually rotated. In this way, the total topological charge of our composite polychromatic beam averages out, and its “hidden” vortex structure cannot be revealed in the total intensity distribution in Fig. 5(a). This means that instead of the expected generation of double charge polychromatic vortex beam, the use of the monochromatic wave plates leads to generation of a complex *topologically mixed* singular beam. Importantly, our method of a simple spectrally resolved cylindrical focusing

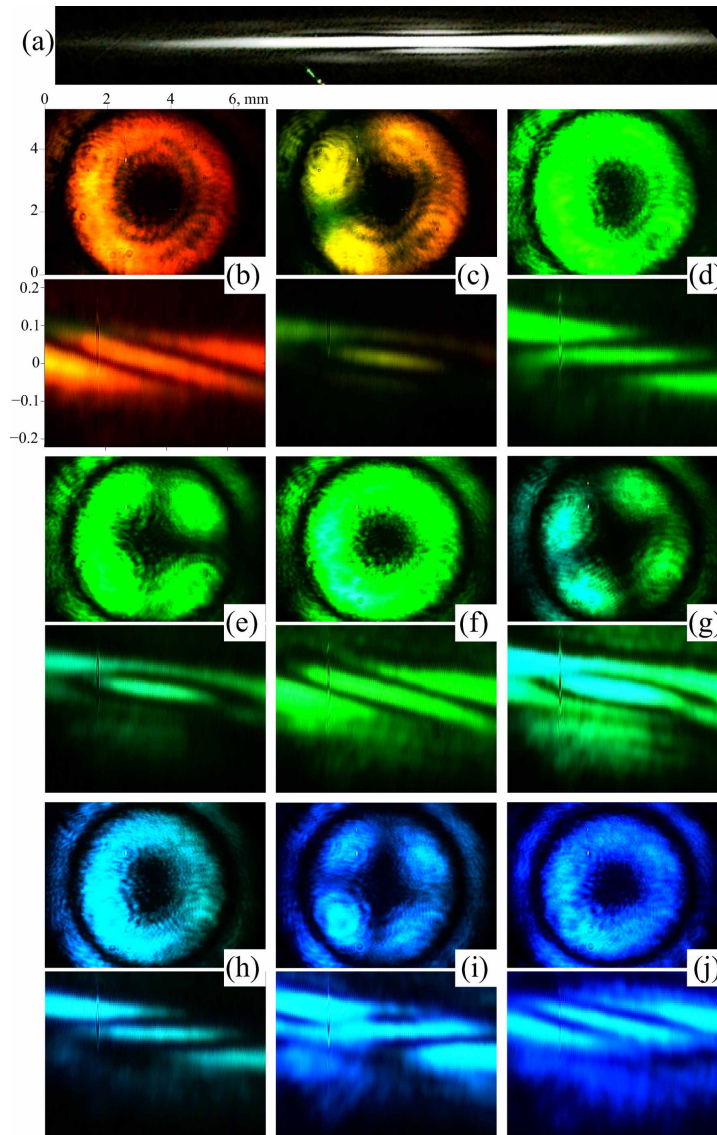


Fig. 5. True color intensity distribution of the polychromatic beam (a) and its spectral components (b-j) without the cylindrical lens (top rows) and in its focal plane (bottom rows). The vertical stretching of the latter is indicated by the spatial scales in (b).

allows to reveal the true topological structure of such beams.

In conclusion, we have demonstrated a simple single-beam experimental technique to determine the topological charge of polychromatic vortex beams. We have applied this method to analyze single- and double-charge vortex beams, as well as a composite singular beam with different topological charges in different spectral components. Noteworthy, in both latter cases, the polychromatic beams have similar intensity distributions while their topological contents are drastically different. Thus, the method presented here can be used as an express diagnostic tool to resolve the spatial structure of complex beams without resorting to multiple beam interferometric experiments.

This work has been supported by the Australian Research Council.